Optimized Low Thrust Trajectories Compared to Impulsive Trajectories for Interplanetary Missions

Aaron M. Schinder *

Solving for preliminary high thrust spacecraft trajectories can be accomplished by simple patched-conic methods. High thrust spacecraft propulsion is limited in Isp to 450 sec for chemical propulsion, and 850 sec for nuclear-thermal propulsion. Electric propulsion thrusters allow much higher Isps (1500-4000 sec), and have enabled high Δv interplanetary missions (10+ kps), as well as interplanetary missions requiring large payload fractions. However, electric propulsion thrusters, even future schemes with very high powers, produce low thrust relative to the powerplant or spacecraft mass, and so traditional patched-conic methods won't produce realistic trajectories or windows for vehicles using them. This work explores the design and optimization of low thrust trajectories and compares them to high thrust trajectories for a simple mission.

I. Introduction

Spacecraft accelerate by use of the rocket principle. There are limited exceptions to this, such as solar sails, or electrodynamic tethers, but most space vehicles in most applicable situations maneuver by expelling propellant at a large velocity. How large the exhaust velocity of the propellant jet is determines how efficiently a spacecraft can maneuver. This relationship is expressed in Tsiolkovsky's rocket equation in the Background section.

Spacecraft rocket propulsion can be broadly divided into classes based on where the energy to accelerate propellant comes from, and subclasses in how the propellant is accelerated. These categories are described in greater detail in the next section. Propulsion systems tend to be either high or low thrust. For high thrust propulsion systems, acceleration takes place over a very short portion of the flight, and the majority of the trajectory is spent under the influence of gravity only. Patched-conic methods, which assume the spacecraft accelerates abruptly between two-body conic section orbits, then coasts along those orbits, can be used to design missions for high thrust vehicles.

Low thrust vehicles must accelerate for large portions of the flight-path. Simple two-body patched conic methods cannot be used to plan low-thrust trajectories. In order to design trajectories for low-thrust vehicles, optimization methods must be used to find acceleration strategies that meet the boundary conditions of the trajectory (departure and arrival position and velocity), and minimize the total cost of the acceleration (mass expended, or integrated power).

II. Background

II.A. Rocket Propulsion Overview

Tsiolkovsky's rocket equation, eq-1, relates the amount of mass that must be expended by a spacecraft in a gravity free or impulsive maneuver to make a certain change in velocity, or Δv. Δv is the total change in velocity of the maneuver. m_0 is the initial mass. m_f is the final mass. v_e is the speed of the propellant jet, equal to Earth's surface gravity times specific impulse, or Isp in sec. In other situations, Δv, rather than being the true change in velocity, can be found to be the integrated thrust/mass (acceleration due to the propellant jet) of the maneuvering spacecraft.

$$m_f/m_0 = exp(-\Delta v/v_e) = exp(-\Delta v/Isp * g_0) \tag{1}$$

*NDSEG Fellow, Department of Aerospace Engineering, 270 Ferst Drive Atlanta GA 30332-0150, AIAA Member.

Many different types of propulsion using the rocket principle have been developed over centuries. For spacecraft, rocket propulsion can be broadly divided into classes based on where the energy to accelerate the propellant comes from. Chemical rockets are powered by chemically reacting the propellant. The specific energy of the chemical reaction limits the specific energy of the propellant jet, and hence the Isp attainable by these rockets. The propellant choice, within very narrow limits, defines the Isp, which is seldom higher than 450 sec in vacuum. Nuclear thermal rockets are a promising technology for massive interplanetary vehicles. These rockets use a nuclear reactor to heat a low molecular mass (usually hydrogen) propellant, and can achieve higher Isps than chemical propulsion. For nuclear propulsion, the limiting factor is the reactor temperatures. Historical tests of nuclear thermal rockets have achieved Isps of 850 sec.[1] These Isp limitations mean that for interplanetary missions, where Δvs of 10s of km/sec are not unusual, large propellant mass fractions, or staging, are required for the spacecraft.

II.B. Overview of EP Engines and Missions

Electric propulsion systems differ from chemical rockets in that an external electric power source is used to accelerate a propellant. Acceleration is usually achieved by ionizing the propellant and manipulating it via electric and magnetic fields. The external nature of the power source means that any amount of specific energy desired can be added to the propellant, enabling much higher Isps to be obtained. Ion drives can operate in the range of 2500 to 4000 sec Isp. Hall effect thrusters have historically operated between 1500 and 2000 sec.[2] For a fixed power limit, there is a tradeoff between thrust and Isp. Current electric propulsion devices have been designed for missions with only a few kW of power, so thrusts tend to be low. Thrusts on the order of 100 - 300 mN for ion drives, and 80-300 mN for Hall thrusters are typical[3456].[7]

Future missions carrying people or cargo may use higher power propulsion schemes, such as magneto-plasmadynamic rockets (MPDs) or designs such as VASIMR (which uses a magnetic nozzle to confine plasma which is heated by an RF antenna). For VASIMR, 200 kW thruster powers have been achieved in the lab, for Isps of 3500 sec, at efficiencies of 54%.[8]

Table 1 shows examples of EP thrusters and their capabilities. Table 2 shows missions beyond Earth which have used EP thrusters as their primary propulsion system.

Table 1. Examples of Electric Propulsion Thrusters and Performance

Engine	Engine Type	Power (kW)	Thrust (mN)	Isp (sec)	Exo-Earth Missions	Source
NSTAR	Ion Drive	2.52	92	3120 to 1700	Deep Space 1, Dawn	3
NEXT	Ion Drive	6.9	236	4190		4
PPS-1350G	Hall Thruster	1.2	70-90	1700	SMART-1	5
BPT-4000	Hall Thruster	3-4.5	170-291	1600-2020		6
SPT-100	Hall Thruster	1.35	85	1600		7
VASIMR	Helicon/Magnetic Nozzle	200	~1500	3500+		8

Table 2. List of EP using Exo-Earth Missions

Misson	Launch Date	Engine	Target
Deep Space 1	1998	NSTAR	Comet Borrelly
Hayabusa	2003	4x Xenon Ion Engines	Asteroid Itokawa Sample Return
SMART-1	2003	PPS-1350G	Moon
Dawn	2007	NSTAR	Ceres and 4 Vesta

Even future high power electric propulsion missions will have low thrusts relative to the mass of the spacecraft. To design trajectories for these vehicles, trajectory optimization routines to solve for the acceleration histories will be necessary.

II.C. Overview of Trajectory Optimization

A general overview to the problem of trajectory optimization is given by Bett's 1998 survey paper.[9] The general trajectory optimization problem can be thought of as follows: Given a trajectory $\vec{y}(t)$, subject to a certain dynamic law, find a control input history $\vec{u}(t)$, for which the trajectory meets certain problem constraints, and for which it minimizes an objective functional $J[\vec{x}(t), \vec{u}(t)]$.

Betts begins his discussion of optimizing a trajectory by providing equations for the objective functional J, Φ, which is a cost function dependent only on the final state, and Ψ which is a boundary condition constraint on the final state. Betts only considers objective functionals dependent on the final state in the derivation of his control equations, though the methods to solve these problems, such as direct shooting, can be generalized to any functional.

$$
\begin{gathered}
J = \Phi(\vec{y}(t_f), t_f) \\
\vec{y} = \vec{f}(\vec{y}(t), \vec{u}(t), t) \\
\Psi[\vec{y}(t_f), \vec{u}(t_f), t_f] = 0
\end{gathered}
\tag{2}
$$

In order to meet the boundary constraints, Lagranges method of undetermined multipliers is used to construct an augmented functional $\hat{J}$. The augmented functional for the case of continuously indexed parameters (the functions $\vec{y}(t)$ and $\vec{u}(t)$) is very similar to the augmented objective function $\hat{F}$ in the case of a set of discrete parameters. $\vec{\nu}$ are a set of discrete lagrange multipliers associated with the boundary condition Ψ. $\vec{\lambda}(t)$ are a set of continuous multiplier functions that constrain the trajectory to follow the dynamic laws of motion.

$$
\hat{J} = [\Phi + \nu^T \Psi]_{t_f} + \int_{t_0}^{t_f} \lambda^T(t)[f(y(t), u(t)) - \dot{y}] \tag{3}
$$

$\lambda^T(t)[f(y(t), u(t)) - \dot{y}]$ is called the optimal control Hamiltonian H. Minimizing the augmented objective functional yields a set of Euler-Lagrange equations, which govern the evolution of the state and lagrange multipliers.

Methods for the solution of the trajectory optimization problem can be divided into two categories: Direct methods, and indirect methods. Direct methods optimize trajectories by operating on $\vec{u}(t)$ or some parameterization thereof. Indirect methods optimize trajectories by operating on $\vec{\lambda}(t)$, and solving for the control variables indirectly.

One direct method algorithm for trajectory optimization, direct shooting, has been widely used in trajectory problems. The algorithm for direct shooting can be stated briefly as follows:

$$
\begin{gathered}
J = J[y(t), u(t; p_i)] \\
\vec{u}(t) = \vec{u}(t; p_1, p_2, ..p_i) \\
g_i(\vec{y}(t_c)) = 0 \\
\vec{y} = \vec{f}(\vec{y}(t), \vec{u}(t), t)
\end{gathered}
\tag{4}
$$

Given an objective function, a finite parameterization governing the form of the control function $\vec{u}$, a set of equality constraints g_i, and a dynamic law governing the state of the trajectory, given $\vec{u}$, do the following:

Choose some initial parameterization $\{p_i\}$;
while *While* $\hat{J}$ *is not converged* **do**
  Perform Newton's Method on $\hat{J}(p_i, \lambda_i)$;
  Inner Loop:;
    For each call to $\hat{J}(p_i, \lambda_i)$, decode what the parameters mean for $\vec{u}(t)$;
    Integrate the trajectory $\vec{y} = \vec{f}(\vec{y}(t), \vec{u}(t; p_i), t)$ from t_0 to t_f;
    Calculate the objective function J;
  Calculate the value of the constraint functions;
  $g_j(\vec{y}(t_c))$;
  Update search direction based on $J(p_i)$ and $g_j(p_i)$.
end
Result: p_i that satisfy g_j and minimize J

Algorithm 1: Direct shooting method algorithm

The direct shooting method has been widely used. Other methods mentioned, such as indirect shooting (which involves optimizing the intial time lagrange multipliers as the problem variables), requires initial guesses to be very close to the final trajectory to converge.[9] Table 3 shows several trajectory optimization programs, and the methods which they use to solve the constrained optimization problem: POST is a Martin Marietta program used for the Titan launch vehicle trajectories. Variants of SEPTOP were used in the planning of the Deep Space 1 trajectory. MALTO is a more modern tool capable of handling more complicated trajectories. MALTO works by dividing the trajectory into segments, fixing the time for each node of the segment, and optimizing impulsive approximations for thrust for each segment, using a two-body Earth-sun approximation.

Table 3. List of optimization programs and the methods they use.

Program	Full Name	Method	Source
VARITOP	Variational Calculus Trajectory Optimization Program	Indirect Method	
SEPTOP	Solar Electric Propulsion Trajectory Optimization Program	Indirect Method	10
MALTO	Mission Analysis Low-Thrust Optimization	Multiple Shooting	11
POST	Program to Optimize Simulated Trajectories	Direct Shooting	9
GTS	Generalized Trajectory Simulation	Direct Shooting	9

In the case of a spacecraft trajectory optimization problem, the functional to minimize is either the total Δv of the spacecraft ($\int |u(t)|/m dt$), hence the mass that must be expended to maneuver, or some function thereof, such as the integrated jet power $\int |\vec{u}(t)|^2 dt$ which minimizes mass in variable specific impulse situations. To compare the results of a low-thrust optimization to the high-thrust Gauss problem, the constraints will be that the spacecraft must end up at the destination (target planet or object) $\vec{y}(t_f) = \vec{r_f}$, at the specified time, with the same velocity as the target planet $\dot{\vec{y}}(t_f) = \vec{v_f}$. The dynamics are acceleration due to gravity, the acceleration due to thrust $\vec{u}(t)/m(t)$, and the loss of mass $\dot{m} = -|u(t)|/Isp/g_0$.

III. Approach

A solar system model was constructed, and routines from *Fundamentals of Astrodynamics* were used to solve for high-thrust two-impulse interplanetary trajectories. A direct shooting algorithm was implemented in Matlab. This shooting method (and the model of the solar system) was validated by reproducing a comparable trajectory to that used by the Dawn mission in it's Ceres-Vesta transfer. The solver was used to study low-thrust trajectories, and compare properties of these trajectories to the impulsive maneuvers for Earth-Mars transfers.

III.A. Two-Body Hierarchal Solar System Model

Several routines from Bate, Mueller, White's *Fundamentals of Astrodynamics* were organized and used to construct a model of the solar system.[12] This model uses unperturbed two-body orbit dynamics to model the bodies of the solar system in a tree-format. Child objects (moons and spacecraft) orbit parent objects (planets, and ultimately the Sun, which is treated as fixed) within the sphere of influence of the parent. Spheres of influence are calculated according to the method given in Prussig and Conway, chapter 9.[13]

$$r_{SOI} = (\frac{m_p}{m_s})^{2/5} r_{sp} \tag{5}$$

Keplerian orbit elements for the planets and moons were taken from JPL's Solar System Dynamics Group's website[14].[15] These elements were given, in the case of the planets, in terms of ecliptic Keplerian elements, and evolution rates of the elements in degrees/century, or rate/century. These elements are strictly valid until 2050 AD, but the rate of evolution is so slow, and the adjustments so small, that for mission trade-study purposes this accuracy won't be necessary. The moon orbit elements and element rates are given in either ecliptic or equatorial coordinates, depending on the object.

Routines for the following tasks have been produced:

1. Julian day to calendar date conversion

2. Orbit elements to position and velocity calculation
3. Universal time of flight problem
4. Gauss problem with p-iteration solver
5. Mean, eccentric, hyperbolic, and true anomaly conversion
6. Solar System state at epoch calculator
7. Porkchop plot generation for high thrust inter-object trajectories

Figure 1 shows a plot of the solar system, for the date 3 Sep 2022, showing a calculated high thrust, low Δv trajectory from Earth to Mars. The positive x-axis through the sun shows the direction of the Vernal equinox. Positions are plotted in the ecliptic plane from ecliptic north.

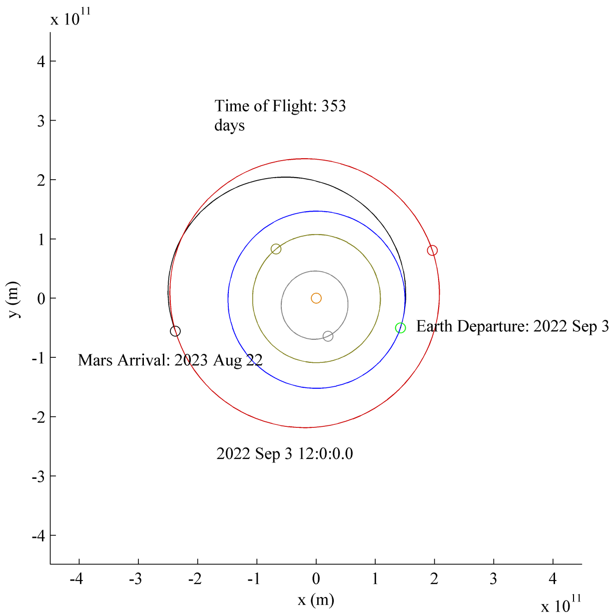

Figure 1. Solar System, 3 Sep 2022 with Earth-Mars Trajectory

III.B. The Direct Shooting Method Solver

A direct shooting method solver has been developed for the optimization of low-thrust trajectories. This solver, in the inner loop, propagates a spacecraft trajectory given the initial position r_0 and velocity v_0, an initial thrust arc shutoff time tt_0, a final adjustment thrust arc start time tt_f, and lists of azimuths and elevations for pointing the thrust vector. This list $\{tt_0, tt_f, az1, el1, az2, el2, ...\}$ constitute the parameters of optimization p_i.

The pointing of the spacecraft's thrusters is interpolated using linear mixing of the resulting control-point vectors, and normalization.

For the outer loop of the direct shooting method: The optimization parameters (the thrusting times and pointing directions), must be adjusted until the trajectory meets the constraint of matching the target objects position and velocity $r_{traj}(t_f) = r_f$, $v_{traj}(t_f) = v_f$. In addition, the solver must choose parameters that minimize the propellant and energy costs of the maneuver.

Because of the way the trajectory is parameterized (the engine is either full on or full off), minimizing either the total maneuver Δv, or the integrated specific thrust power will yield the same minimum. In a variable thruster specific impulse, or a variable mass-flow situation, the choice of either Δv or energy will have an impact on the eventual solution.

Several variants of a method to solve this problem were tried. One method to handle the constraints is the use of Newton's method to solve a constrained optimization problem, as shown in the previous section.

The method eventually chosen was to use a positive definite augmented objective function, and to search for a minimum using a Conjugate Gradient search. The augmented objective function has a penalty function imposed for failing to meet final position and velocity constraints. The form of this penalty function (quadratic in scaled position and velocity error) causes the search to favor solutions that meet the final constraints.

For this method, the augmented objective functional is the following. k_{c1} and k_{c2} are penalty multipliers chosen so that not satisfying the final position and velocity is heavily penalized (large, but not so large that the solver does not converge):

$$J = \int_{t_0}^{t_f} |u|(t) dt \hat{J} = \int_{t_0}^{t_f} |u|(t) dt + k_{c1} * (|\vec{r_f} - \vec{y}(t_f)|^2) + k_{c2} * (|\vec{v_f} - \dot{\vec{y}}(t_f)|^2) \tag{6}$$

The updated algorithm is roughly the same, without the Lagrange multipliers:

Choose some initial parameterization $\{p_i\}$;

while *While* $\hat{J}$ *is not converged* **do**

Perform CG linesearch to minimize $\hat{J}(p_i)$;

Inner Loop:;

For each call to $\hat{J}(p_i)$, decode what the parameters mean for $\vec{u}(t)$;

Integrate the trajectory $\dot{\vec{y}} = \vec{f}(\vec{y}(t), \vec{u}(t; p_i), t)$ from t_0 to t_f;

Calculate the objective function $\hat{J}$;

Update search direction based on $J(p_i)$

end

Result: p_i that satisfy g_j and minimize J

Algorithm 2: Updated algorithm

The advantage of the Conjugate Gradient search is that it is much faster than Newton's method. CG only has to compute a full gradient of the objective function once per iteration, and does not need to compute a Hessian. For expensive objective function evaluations (the inner loop of the shooting method requires integrating a full trajectory at each variation of the objective function) this leads to much faster iteration. CG is also stable, provided the objective function is positive definite, or has strict minima in the region being searched.

This method is also important, in that inequality constraints can be handled in the same way as the equality constraints: By imposing a variably scaled addition to the cost function.

Given an inequality constraint:

$$g(\vec{x}) > 0 \tag{7}$$

You can construct a positive definite L2 continuous function which applies a penalty only when the solution wanders into it's zone of exclusion. This can be added to the objective function.

$$C(\vec{x}) = max(0, g(\vec{x}))^2 \tag{8}$$

III.C. Validation: Comparison of Solver Solution with Dawn Trajectory Arc

In order to validate that the direct shooting method solver is producing reasonable solutions, the output is compared to a trajectory from an EP enabled interplanetary mission. The Vesta-Ceres interplanetary transfer trajectory given in Brophy[16] is compared with the output of the shooting method solver for a similar physical situation.

The Dawn spacecraft has an initial (wet) mass of 1240 kg. Of that, 450 kg are the Xenon fuel for the ion engines. Dawn has three gimbaled NEXT ion thrusters, each capable of producing 92 mN of thrust. Presumably the maximum acceleration at the initial mass of which the spacecraft is capable is 0.22 mm/sec^2. If only one engine is used, it is 0.073 mm/sec^2.

The trajectory depicted in Brophy[16] shows thrusting for the majority of the transfer arc, indicating that a lower thrust than the engine maximum is being output. Dawn leaves Vesta on May 2012, and arrives at Ceres on August 2015.

Using 200 timesteps per shot, four control points for the initial and final maneuver thrust directions, and a thrust corresponding to an initial acceleration capability of 0.073 mm/sec^2, a comparable trajectory is obtained. The total Δv is 2730 m/sec, and the total integrated specific thrust power is 0.2067 m^2/sec^3. This trajectory meets position and velocity constraints to within 0.15% and 2.62% of Ceres's orbital position and velocity. (For comparison, the initial guess trajectory, based on spreading out an impulsive maneuver to finite thrust times, did not reach Ceres at all (90+% errors).)

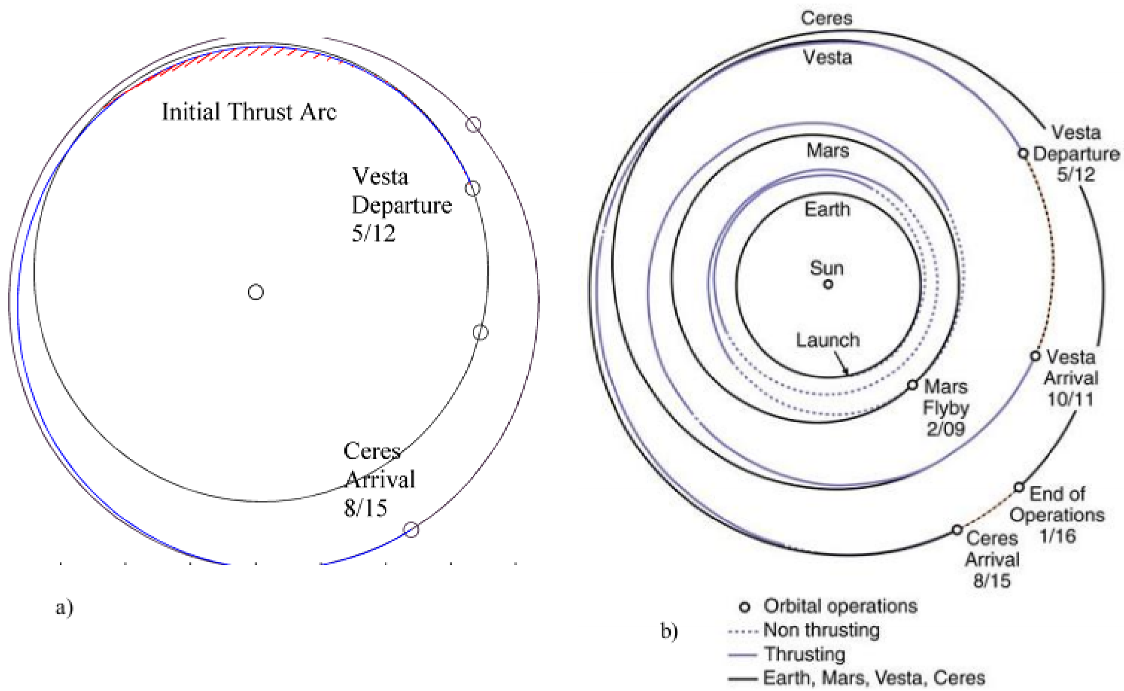

Figure 2. a) Shooting method converged trajectory, b) Dawn trajectory, from Brophy[16]

The depicted thrust vectors are mostly out of the ecliptic plane. The majority of the Δv generated by this method is applied to changing the plane of Dawn's orbit. This is shown in Figure 3.

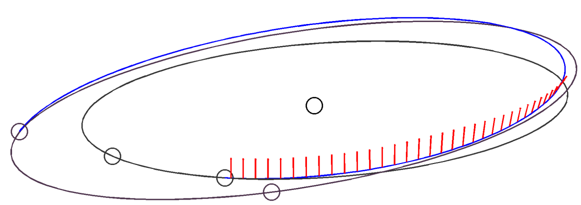

Figure 3. Thrust vector components out of ecliptic plane

The convergence of the shooting method is shown in Figure 4. The value for the objective function relative to the last iteration (which is taken to be the minimum for this analysis) is plotted versus the CG solver iteration.

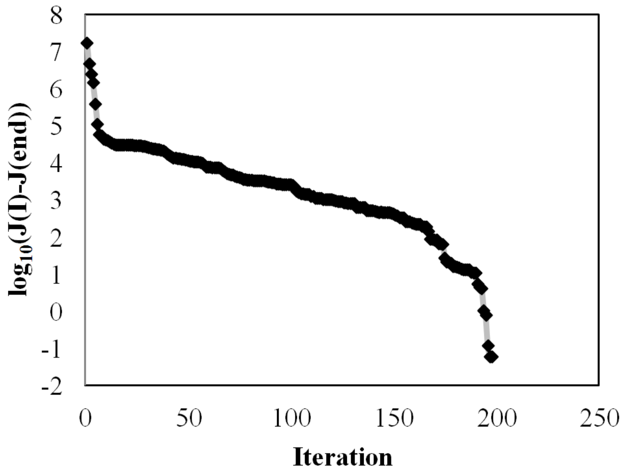

Figure 4. Relative convergence of objective function vs. CG solver iteration

This analysis demonstrates that reasonable trajectories result from the low thrust trajectory solver. Similar behavior is seen in both the trajectory chosen by JPL, and the trajectory generated by the direct-shooting solver.

IV. Results

A model of the solar system was constructed, and Gauss's problem was solved for

IV.A. High Thrust Earth-Mars Trajectories

For a fixed time of departure from Earth, and time of arrival at Mars, the Gauss problem (finding a two-body solar orbit linking $r_{\vec{Earth}}$ at departure and $r_{\vec{Mars}}$ at arrival, yields only two solutions. These solutions, a type I orbit with a change in true anomaly about the sun less than 180deg, and a type II orbit, with a larger than 180deg true anomaly change, each have different Δvs with respect to the initial and final orbital velocities of Earth and Mars. The total Δvs are functions of the departure and arrival time. By choosing the lowest Δv orbit, a plot of Δv for arrival and departure times for the case of a two-impulse transfer can be generated. This plot is called a "Porkchop Plot", and usually contains minima lobes every synodic period of the two objects being traversed.

Using the Gauss problem solver and the model of the solar system, porkchop plots for the delta-V of high-thrust impulsive maneuvers were calculated for departing Earth in summer 2022, and shown below in Figure 5. Figure 1 shows a representative Earth-Mars trajectory during this timeframe.

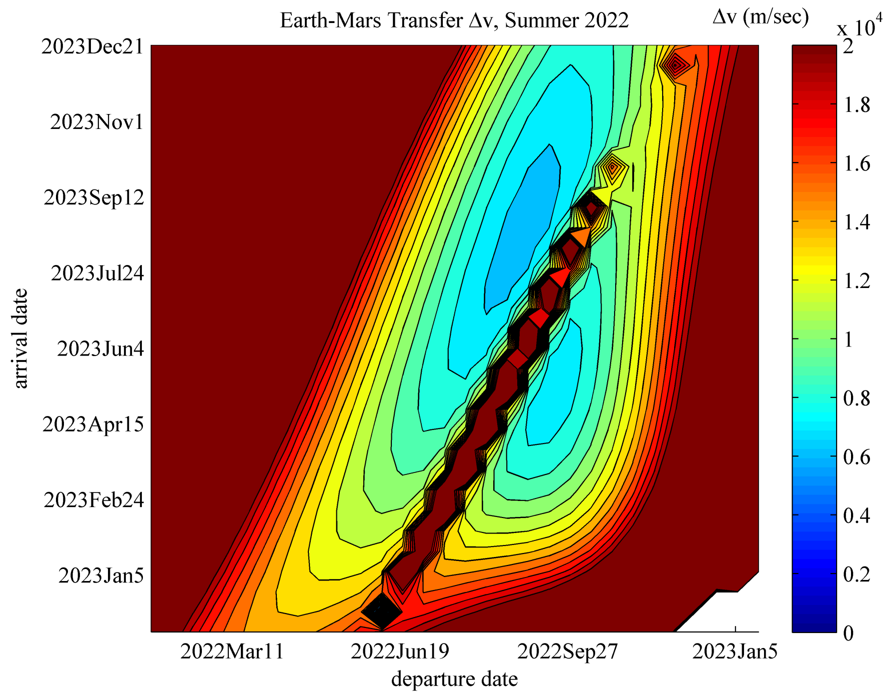

Figure 5. Porkchop plot for best conic-section Earth-Mars transfer Δv, summer 2022

IV.B. Low Thrust Earth-Mars Trajectory Comparison

For low thrust trajectories, using only 200 timesteps per trajectory integration and 3 control points each for the thrust direction for the initial and final thrust arcs are used to navigate between Earth and Mars. By appropriately scaling the penalty functions, solutions that meet the final position and velocity of Mars to within 1% and 5% respectively can be found. One representative trajectory is shown in Figure 6.

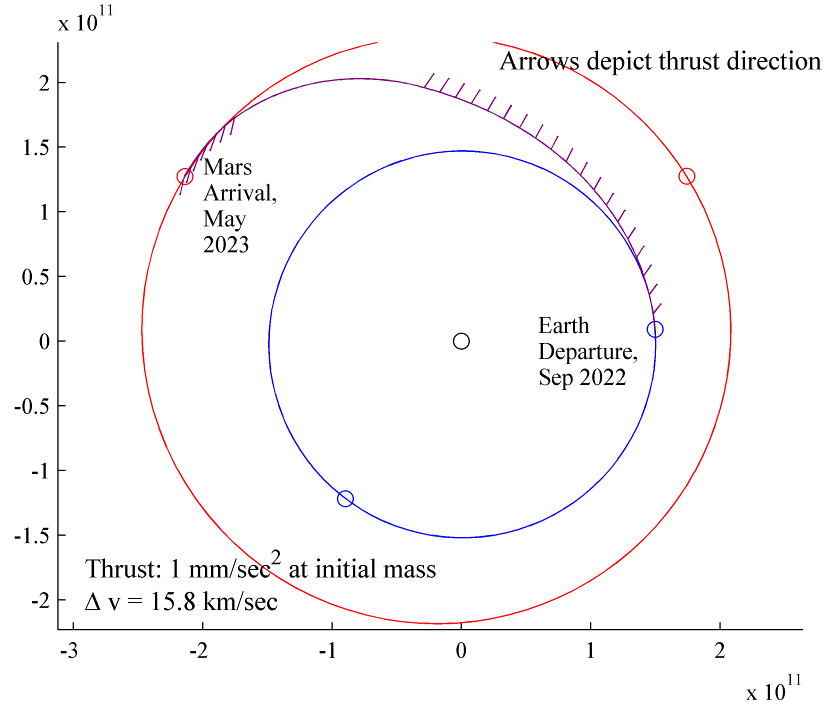

Figure 6. Representative low thrust Earth-Mars trajectory

For missions assuming a thrust capability providing 1 mm/sec^2 of acceleration at initial mass, and 3000 sec Isp, a pareto front of trajectories were calculated for departing Earth on 1 Aug 2022, and arriving at Mars at varying times over the course of the next 1.5 years. These are the blue circle solutions in the figures below.

To verify that this pareto front was well converged, the number of control points per thrust arc was increased to 4, and the timesteps were doubled (Blue and red diamonds). A similar pareto front was calculated for an initial mass thrust yielding 0.5 mm/sec^2 acceleration (Green diamonds). Trajectories that arrived at the target planet with less than 1% position and 5% velocity error are shown. Gaps are where convergence was not obtained.

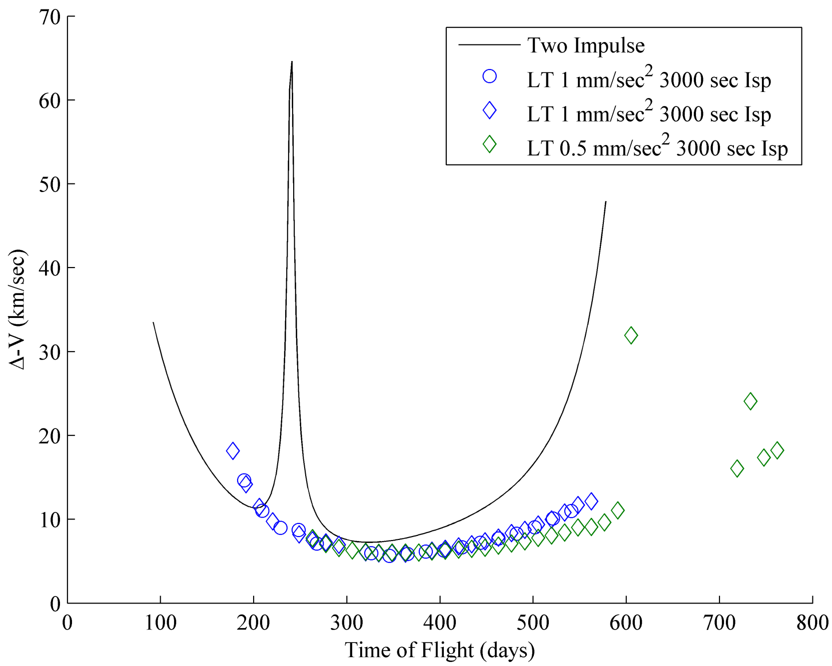

Figure 7. Δvs for Earth-Mars flight beginning 1 Aug 2022: Comparison of two-impulse with low-thrust trajectories

Figure 7 shows a comparison of delta-Vs for each of these scenarios described above, and is compared to the 1-Aug departure slice of the porkchop plot in Figure 5. The low-thrust trajectories are generally able to converge to lower Δv solutions than the two-impulse case, where the acceleration is entirely constrained by the departure and arrival times. The greater degrees of freedom in thrusting time and duration allow the solver to seek a better trajectory. Other optimization problems could be created for multiple-impulse trajectories that would probably produce slightly lower Δvs still, though there is a limit to how much it can be minimized given the problem constraints and no other perturbations such as gravity assists.

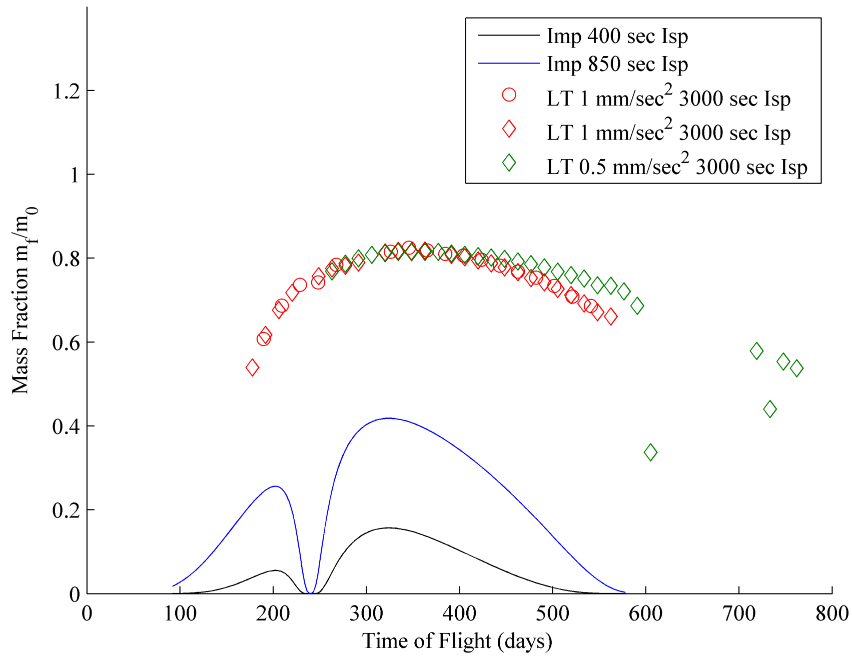

Figure 8. Comparison of final mass-ratios for different Isp scenarios

The mass fractions obtainable with the higher Isp EP engines are much higher than for chemical propulsion (450 sec case) and nuclear thermal rockets (850 sec case). For nuclear thermal rockets, 50% propellant mass is about the best you can do with this launch date. For a round-trip, a nuclear-thermal rocket would need more than 75% propellant mass fraction to be able to make the maneuvers. EP thrusters, assuming an Isp in the 3000 sec range, can have more than 80% useful payload and structure!

Low thrust missions are not significantly less flexible than two-impulse missions in terms of their launch windows either, provided you can accelerate at a high enough rate. For the 1 mm/sec^2 case, solutions did not begin converging until around 180 days travel time: If there is too little time to accelerate, the required velocity changes cannot be made by low thrust engines. For the 0.5 mm/sec^2 case, solutions did not begin to converge until 250 days travel time. The minimum travel time is one important limit on the capability of these thrusters.

V. Conclusions

A low thrust trajectory optimizing routine was created to explore the possibilities for low-thrust, high-Isp electric propulsion engines to make interplanetary maneuvers. Interplanetary flights are characterized by high Δv requirements, but flight times are long enough that low accelerations over long periods of time can achieve interplanetary transfers with reasonable flexibility. High Isp is important, as mass fractions are much higher for EP spacecraft, and Δv s are not significantly higher for the low-thrust trajectories than for two-impulse transfers. Low thrust trajectories for a 1 mm/sec^2 and 0.5 mm/sec^2, 3000 sec Isp EP thruster, were compared to two-impulse chemical and nuclear thermal rockets for one leg of an Earth-Mars mission, and the low thrust trajectories converged for travel times in the range of the longer type-II two-impulse trajectories. Electric propulsion is an important enabling technology for interplanetary spaceflight, and low thrust optimization is an important capability to plan these missions.

References

[1]Finseth, J. L., "Rover nuclear rocket engine program: Overview of rover engine tests. Final Report," Tech. rep., Sverdrup Technology, Inc., Huntsville, AL (United States), 1991.

[2]Goebel, D. M. and Katz, I., *Fundamentals of electric propulsion: ion and Hall thrusters*, Vol. 1, Wiley. com, 2008.

[3]Polk, J. E., Kakuda, R. Y., Anderson, J. R., Brophy, J. R., Rawlin, V. K., Patterson, M. J., Sovey, J., and Hamley, J., "Validation of the NSTAR ion propulsion system on the Deep Space One mission: overview and initial results," *AIAA paper*, Vol. 99, 1999, pp. 2274.

[4]Patterson, M. J., "NEXT Study of Thruster Extended-Performance II (NEXT STEP II)," *Paper AIAA*, Vol. 4808, 2008.

[5]Marchandise, F. R., Biron, J., Gambon, M., Cornu, N., Darnon, F., and Estublier, D., "The PPS-1350 qualification demonstration 7500h on ground, about 5000h in flight," *29th International Electric Propulsion Conference, IEPC Paper*, Vol. 209, 2005.

[6]Kristi de Grys, Christopher Rayburn, Fred Wilson, Jack Fisher, Lance Werthman, and Vadim Khayms, "BPT-4000 Multi-Mode 4.5 KW Hall Thruster Qualification Status," *39th AIAA/ASME/SAE/ASEE Joint Propulsion Conference and Exhibit*, Joint Propulsion Conferences, American Institute of Aeronautics and Astronautics, 2003.

[7]Charles Garner, John Brophy, James Polk, and Lewis Pless, "A 5,730-hr cyclic endurance test of the SPT-100," *31st Joint Propulsion Conference and Exhibit*, Joint Propulsion Conferences, American Institute of Aeronautics and Astronautics, San Diego, CA, July 1995.

[8]Cassady, L. D., Longmier, B. W., Olsen, C. S., Ballenger, M. G., McCaskill, G. E., Ilin, A. V., Carter, M. D., Glover, T. W., Squire, J. P., and Daz, F. R. C., "Vasimrr performance results," *46th Joint Propulsion Conference*, 2010.

[9]Betts, J. T., "Survey of numerical methods for trajectory optimization," *Journal of guidance, control, and dynamics*, Vol. 21, No. 2, 1998, pp. 193–207.

[10]Sims, J. A. and Flanagan, S. N., "Preliminary design of low-thrust planetary missions," 1997.

[11]Sims, J. A., Finlayson, P. A., Rinderle, E. A., Vavrina, M. A., and Kowalkowski, T. D., *Implementation of a low-thrust trajectory optimization algorithm for preliminary design*, Pasadena, CA: Jet Propulsion Laboratory, National Aeronautics and Space Administration, 2006.

[12]Bate, R. R., Mueller, D. D., and White, J. E., *Fundamentals of astrodynamics*, Courier Corporation, 1971.

[13]Prussing, J. E. and Conway, B. A., *Orbital mechanics*, Oxford University Press, USA, 1993.

[14]Standish, E., "Keplerian Elements for Approximate Positions of the Major Planets," .

[15]"Planetary Satellite Mean Orbital Parameters," .

[16]Brophy, J. R., Ganapathi, G. B., Garner, C. E., Gates, J., Lo, J., Marcucci, M. G., and Nakazono, B., "Status of the Dawn Ion Propulsion System," *AIAA paper*, Vol. 3433, 2004.

A. An Alternative Parameterization for Low Thrust Optimization

An alternative parameterization for low thrust optimization (than the shooting method) can be made: If the trajectory is treated as a segmented series of cubic-splines, then the positions of control points, distributed in various ways in time between initial and final time, determine the shape of the trajectory. The acceleration can be calculated at the midpoint and control points of each spline, and the acceleration not due to gravity is the acceleration which must be supplied by the thruster.

The variable specific impulse objective function $J = \int |u(t)|^2 * dt$ can be minimized by using unconstrained optimization methods, such as conjugate gradient descent.

Figure 9 shows a trajectory being optimized with this method. Convergence to *some* sort of solution is guaranteed, as there is no way for a trajectory thus parameterized to not meet the final position and velocity conditions, as in the shooting method. However, this solver converged slowly compared with the shooting method, and the Δvs of the final trajectories were not very low for reasonably coarse parameterizations. Perhaps future work could refine the distribution of spline control points.

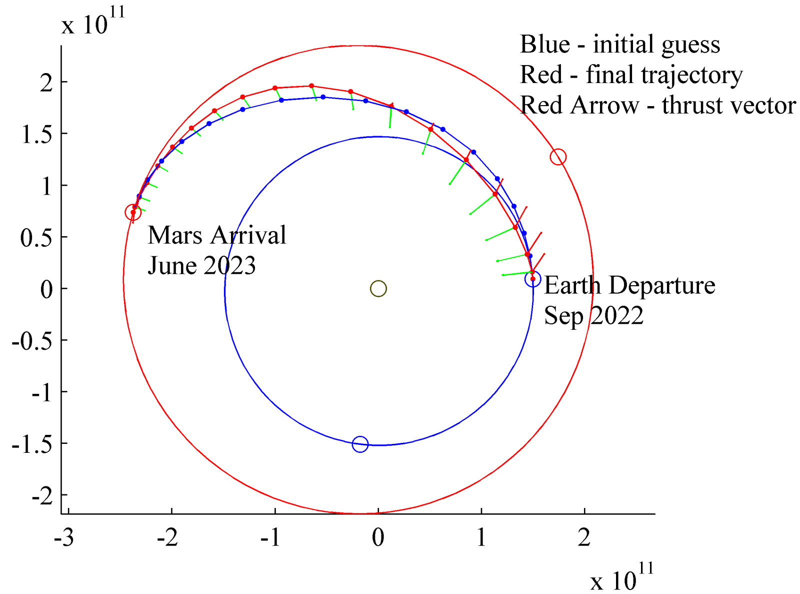

Figure 9. An alternative solver for low-thrust trajectories